CERN-PH-TH/2007-007
hep-ph/0701158
January 22, 2007

Multi-W Events at LHC from a Warped Extra Dimension with Custodial Symmetry

Christopher Dennis[a], Müge Karagöz Ünel[a],
Géraldine Servant [b,c] and Jeff Tseng[a]

[a] *University of Oxford, Subdepartment of Particle Physics, Keble Road, Oxford, OX1 3RH, UK*
[b] *CERN, Theory Division, CH-1211 Geneva 23, Switzerland*
[c] *Service de Physique Théorique, CEA Saclay, F91191 Gif–sur–Yvette, France*

C.Dennis2@physics.ox.ac.uk, karagozm@cern.ch
geraldine.servant@cern.ch,j.tseng1@physics.ox.ac.uk

Abstract

Randall–Sundrum models based on $SU(2)_L \times SU(2)_R$ with custodial symmetry are compelling frameworks for building alternative models of electroweak symmetry breaking. A particular feature of these models is the likely presence of light Kaluza-Klein fermions related to the right-handed top quark. These can be as light as a few hundred GeV and still compatible with EW precision constraints. In this article, we study the detectability of four-W final states at the LHC, which arise from the pair-production and tW decay of light Kaluza-Klein bottom quarks as well as light Kaluza-Klein quarks carrying electric charge 5/3.

1 Introduction

In the last eight years, extra-dimensional models have been suggested to solve the gauge hierarchy problem. Among them, the Randall–Sundrum (RS) model [1] is the most appealing, where the hierarchy between the electroweak (EW) and the Planck scales arises from a warped higher dimensional spacetime. Variants of the original set-up have matured over the years. Eventually, all Standard Model (SM) fields except the Higgs (to solve the hierarchy problem, it is sufficient that just the Higgs –or alternative dynamics responsible for electroweak symmetry breaking– be localized at the TeV brane) have been promoted to bulk fields rather than brane fields. It has been shown that EW precision constraints are much ameliorated if the EW gauge symmetry in the 5-dimensional bulk is enlarged to $SU(2)_L \times SU(2)_R \times U(1)_X$ [2]. The AdS/CFT correspondence suggests that this model is dual to a strongly coupled CFT Higgs sector [3]. Also, the $SU(2)_L \times SU(2)_R$ gauge symmetry in the RS bulk implies the presence of a global custodial isospin symmetry of the CFT Higgs sector, thus protecting EW observables from excessive new contributions [2]. This gauge structure in warped space has also been used to construct Higgsless models of EW symmetry breaking [4].

In this framework, Kaluza-Klein (KK) excitations of gauge bosons of mass $M_{KK} \sim 3$ TeV are allowed (even lower, ~ 500 GeV, for Higgsless models). Generically, the mass spectrum of fermionic KK modes depends on the boundary conditions (BC) imposed on the TeV and Planck branes, localized at the boundaries of the slice of AdS_5. These are commonly modelled by either Neumann $(+)$ or Dirichlet $(-)$ BC in orbifold compactifications. Early studies in Randall-Sundrum background considered Neumann boundary conditions only, in which case all KK masses have to be larger than the gauge boson KK mass of 3 TeV and will be difficult to produce at the LHC. In recent models, different boundary conditions have been imposed, leading to richer possibilities for model building and to the potential presence of light KK fermions, observable at colliders. These fields have for instance Dirichlet BC on the Planck brane and Neumann BC on the TeV brane. They are denoted $(-+)$ KK fermions, and do not have zero modes.

The heaviness of the top quark is explained by the localization of the wave function of the top quark zero mode near the TeV brane, guaranteeing a large Yukawa coupling with the Higgs. In the initial model of Ref. [2], the Right-Handed (RH) top quark is included in a doublet of the $SU(2)_R$ symmetry. Its b_R partner does not have a zero mode but its first KK excitation is expected to be light. This mode mixes with the SM bottom quark and induces large corrections to $Z \to b\overline{b}$, so its mass has to be at least ~ 1.5 TeV [2]. However, it has been recently pointed out in Ref. [5] that the custodial symmetry, together with a discrete $L \leftrightarrow R$ symmetry and alternative $SU(2)_R$ assignments for the top and bottom quarks, can protect the $Zb\overline{b}$ coupling and allow light masses for the KK b_R as low as a few hundreds of GeV. This mode is accompanied by other light degenerate KK quarks (carrying electric charge $Q = 2/3, -1/3, 5/3$), that have been named "the custodians" [6]. They are likely to be the lightest KK states in these models and could be produced at the LHC.

The interesting phenomenology of light $(-+)$ KK fermions was pointed out in Ref. [7] and its extended version Ref. [8], where it was emphasized that light KK fermions are expected as a consequence of the heaviness of the top quark. More precisely, KK partners of the RH top should be light. Even though the study of [7, 8] deals with the embedding of these $SU(2)_L \times SU(2)_R \times U(1)$ Randall–Sundrum models into a GUT[1], the statement remains pretty

[1] In this case, an extra Z_3 symmetry can be imposed to protect proton stability, leading to the stability of

general: $(-+)$ KK partners belonging to the t_R multiplet are expected to be light and can be probed at colliders. The possibility of pair-producing these KK fermions, leading to multi W events, was discussed. Most of these signatures were specific to the GUT model except for the production of the KK b_R (that we denote $\tilde{b}_R$), which is common to a large class of models. In this paper, we focus on the pair production and tW decay of $\tilde{b}_R$, which leads to a very unique $4W + b\overline{b}$ final state. This is a promising signature for probing RS models with custodial symmetry[2]. Moreover, while we will focus on the $\tilde{b}_R$ in this paper, it should be noted that our study applies as well to pair production of other custodians such as the KK b_L and the exotic KK quark with electric charge $Q = 5/3$, that both decay into tW.

The pair production of exotic quarks, singlet under $SU(2)_L$, was considered in the past in Ref. [10]. The single and pair production of heavy T quarks in Little Higgs models was studied in Ref. [11]. However, these quarks have charge +2/3 instead of -1/3 or 5/3, so the decay is into Wb rather than Wt and there are only 2 W's in the event. We are not aware of previous studies investigating events with more than 2 W's in the final state[3]. While 4-W production brings the prospect of a spectacularly rich multi-jet plus multi-lepton signature, distinguishing the signal from backgrounds will still be challenging. Our goal in this paper is to investigate the feasibility of doing so and thus identifying $\tilde{b}_R$ at the LHC.

A straightforward trigger criterion for these events is that of a single, isolated lepton with missing E_T, *i.e.*, the standard leptonic W data stream. Other W's in the event would be reconstructed using dijet pairs. Multi-lepton triggers can also be used. The fermions $\tilde{b}_R$ are particularly accessible, producing b jets which could be tagged with displaced tracks. If one $\tilde{b}_R$ enters the leptonic W data stream, its antiparticle partner is potentially amenable to full reconstruction.

In the present work, we neglect hadronization effects. For the range of masses considered, the width of $\tilde{b}_R$ is large enough that the decay takes place before hadronization.

For low $\tilde{b}_R$ masses (< 300 GeV), there are interconnection effects. This situation is common to nearly all investigations of heavy particles with GeV-scale widths such as WW, ZZ, and $t\overline{t}$ where hadronic decays overlap. We assume this effect is small; this is justified for the $\mathcal{O}(500)$ GeV masses we consider in detail, and we neglect it for now (it is interesting to note that on the opposite extreme, the KK fermions of [8] are very long-lived and lead to CHAMP-like signatures; for these, we are well into the realm of Heavy Quark Effective Theory, so that to first order we can again neglect light quark effects in the decay).

In Section 2, we describe the parameters of the model and the decay channels of $\tilde{b}_R$. Readers who are more keen on the experimental aspects than on the model-building details can skip this section. Section 3 discusses the possible signatures associated with $\tilde{b}_R$ pair production and presents the main SM backgrounds mimicking the $4W$ signature. Section 4 gathers the results of our simulation and outlines a promising strategy for distinguishing the signal from the SM backgrounds using early (10 fb^{-1}) LHC data.

a stable light KK right-handed neutrino.

[2]Collider signatures of this class of models are only starting to be investigated, see for instance [9].

[3]Multiple weak gauge boson production was theoretically investigated in the eighties [12, 13] and early nineties [14–16] in the context of the Superconducting Super Collider (SSC), as these processes were (and are) of great interest to test whether the EW symmetry breaking is due to new strong interactions. If this is the case, multiple (> 2) longitudinal W and Z production would be enhanced at SSC energies [12, 14]. This is nevertheless still a small effect compared to the rates for the standard production of multiple transverse W and Z and it was concluded that it would not be observable [13]. More recent work has suggested that these studies could be performed with $\mathcal{O}(1000)$ fb^{-1} of data that could be delivered by an upgraded LHC [17].

2 Model parameters

Our analysis describes the pair production and decay of $\tilde{b}_R$. However, as we said in the introduction, there are typically other "custodian" quarks which lead to the same $4W$ signature, potentially significantly enlarging our signal. The number of custodians is model-dependent. Following [5], several papers have appeared recently on the phenomenology associated with these light KK fermions [6, 18–20]. These studies consider different embeddings for the SM top and bottom quarks, leading to various possibilities for the number and masses of the custodians. In the description below, we assume for simplicity that there is only one light KK quark, $\tilde{b}_R$, the $SU(2)_R$ doublet partner of the SM RH top quark. This is not the realistic situation but it does not matter for our analysis. At the end of this section, we comment how to generalize our discussion to the more realistic models mentioned above.

KK fermions are 4-component spinors which have both a LH and a RH chirality. One chirality has $(-+)$ BC while the other has $(+-)$. The RH chirality of the KK b_R under consideration turns out to be localized near the TeV brane and the LH one near the Planck brane. Therefore, the couplings of the LH chirality with modes localized near the TeV brane, such as the Higgs, the top quark and KK excitations, are suppressed. In contrast, the direct interactions of KK fermions to zero-mode gauge bosons are vector-like. This is because zero-mode gauge bosons have a flat profile (unlike KK modes) and couple identically to both chiralities of KK fermions. The couplings of the KK b_R to SM gauge bosons are the same as the couplings of the SM b_R quark, except that they involve both chiralities identically. The vertices $\overline{\tilde{b}}_R \tilde{b}_R G_\mu$, $\overline{\tilde{b}}_R \tilde{b}_R A_\mu$ and $\overline{\tilde{b}}_R \tilde{b}_R Z_\mu$ are respectively $g_s\gamma_\mu$, $-e\gamma_\mu/3$ and $e\tan\theta_W\gamma_\mu/3$. $\tilde{b}_R$ has four decay channels: $\tilde{b}_R \to t_R W$, $\tilde{b}_R \to t_L W$, $\tilde{b}_R \to b_L H$ and $\tilde{b}_R \to b_L Z$. The first two lead to the multi W signature we are interested in, while the third can also lead to it if the Higgs decays dominantly into WW. We now present these decays in details.

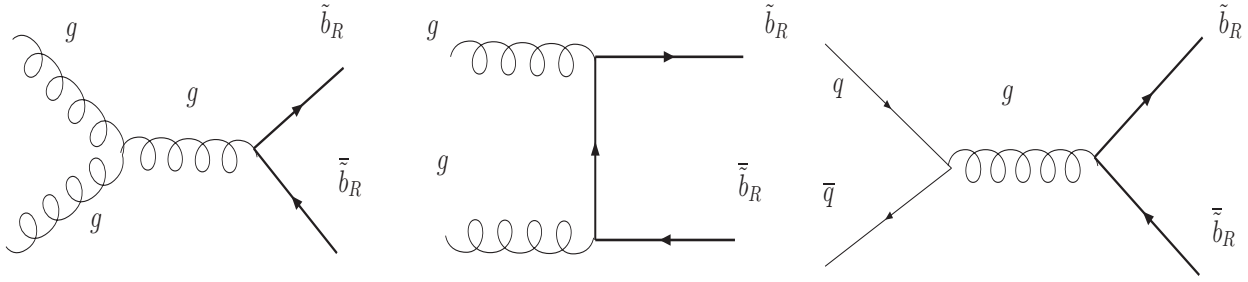

Figure 1: Dominant channels for pair production of $\tilde{b}_R$.

2.1 $\tilde{b}_R \to t_R W^-$ decay

$\tilde{b}_R$, as a singlet under $SU(2)_L$, is not expected to couple to W. The effective coupling of $\tilde{b}_R$ to W is due to $W_R - W_L$ mixing resulting from EW symmetry breaking (see Fig. 3). W_R is the charged gauge boson associated with $SU(2)_R$ and does not have a zero mode. We consider the effect of the mixing of the SM W with the first KK excitation of W_R, which has mass

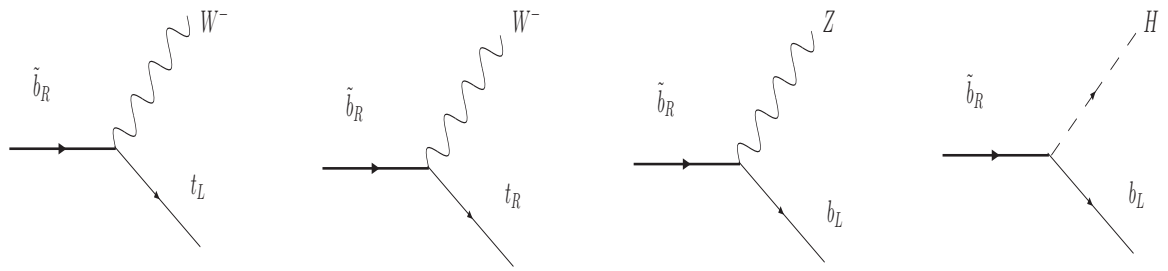

Figure 2: The four decay channels of $\tilde{b}_R$.

$M_{KK} \sim 3$ TeV. The induced coupling is then $g_{\tilde{b}_R,t_R,W^-}\ \gamma_\mu$ where:

$$g_{\tilde{b}_R,t_R,W^-} = \frac{g_R}{\sqrt{2}}\sqrt{k\pi r_c} \times P_R \times \mathcal{M}_{W_R-W_L} \times \mathcal{F}_{\tilde{b}_R,t_R} \quad (1)$$

$$\mathcal{M}_{W_R-W_L} = \frac{g_R}{g}\sqrt{2k\pi r_c}\frac{M_W^2}{M_{KK}^2}. \quad (2)$$

$\mathcal{F}_{\tilde{b}_R,t_R} \sim 1$ is the form factor reflecting the overlap between the wave functions of $\tilde{b}_R$, W_R and t_R. $\mathcal{M}_{W_R-W_L}$ is the mixing factor due to the EW breaking vev of the Higgs. $k\pi r_c = \ln(10^{15})$ is the exponent of the warp factor needed to generate the weak/Planck hierarchy. This formula assumes the Higgs is localized on the TeV brane. If it is delocalized in the extra dimension as in scenarios of gauge-Higgs unification where it is identified with the 5th component of a gauge boson, we can replace the factor $\sqrt{2k\pi r_c}$ with the form factor accounting for the wave function overlap. In this case, using the profile given in [21] (see also Appendix B of [8]) $\sqrt{2k\pi r_c} \approx 8.31$ is replaced by 5.748. P_R is the RH projector that expresses the fact that only one chirality of the KK b_R has a non-suppressed coupling to W_R. g_R is the 4D gauge coupling of $SU(2)_R$. The LR discrete symmetry requires $g_L = g_R$ at 5D level. Since the 5D g_L is fixed by the matching with the 4D g_L (assuming that brane kinetic terms are small), we can replace g_R by g, the SM $SU(2)$ coupling, in the above formulae. As is clear from Fig. 4, this decay is negligible compared to the other three channels.

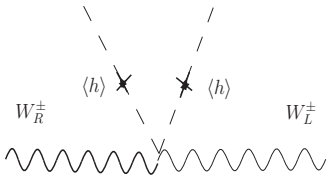

Figure 3: Diagram leading to $W_R^\pm - W_L^\pm$ mixing.

2.2 $\tilde{b}_R \to t_L W^-$, $\tilde{b}_R \to b_L Z$ and $\tilde{b}_R \to b_L H$ decays

The Yukawa coupling between the (t_L, b_L) and $(t_R, \tilde{b}_R)$ multiplets generates three more decay modes for $\tilde{b}_R$: $\tilde{b}_R \to b_L H$, $\tilde{b}_R \to t_L W^-$ and $\tilde{b}_R \to b_L Z$.

The coupling between b_L, H and $\tilde{b}_R$ is $y_t f(c_{t_R})/\sqrt{2}$, where $y_t = 1$ and $f(c) \approx \sqrt{2/(1-2c)}$ (for $c \gtrsim -1/2$) comes from the wavefunction of the RH top quark given in appendix A of [8]. The c-parameter corresponds to the 5D fermionic bulk mass in Planck units. For the right-handed top quark, we take $c = -1/2$, leading to $f(c_{t_R}) = 1$.

The second decay comes from the interaction $\tilde{b}_R.t_L.H^{\pm}$ where $H^{\pm}$ is the would-be Goldstone boson which becomes a longitudinal W. In unitary gauge, there is no $H^{\pm}$, and this has to be written in the form of a γ_μ interaction. However, such an interaction will couple a LH (RH) fermion with a LH (RH) fermion. As we said earlier, the RH chirality of the KK b_R under consideration turns out to be localized near the TeV brane and the LH one near the Planck brane. Therefore, the coupling of the LH chirality with the top quark is suppressed (since the top is localized near the TeV brane). One would be tempted to conclude that there is no coupling between $\tilde{b}_R$ t_L and W, but there is a subtlety: the LH chirality of the *physical* (mass eigenstate) b_R is actually a linear combination of a LH KK b_R and a zero mode b_L. There is some mixing effect (comparable to the one discussed in section 9.3 of [8]) due to the top Yukawa coupling which generates a mass term between b_L and $\tilde{b}_R$. After diagonalization of the mass matrix, we can see that the new mass eigenstate $\tilde{b}_R$ has an admixture of the zero mode b_L, through which it couples to W and Z. Specifically, in unitary gauge,

$$[\text{physical } \tilde{b}]_{LH} = \cos\theta \; \hat{\tilde{b}}_R + \sin\theta \; b_L \tag{3}$$

where $\hat{\tilde{b}}_R$ denotes the LH chirality of KK b_R, and $\sin\theta \approx m_t f(c_{t_R})/m_{\tilde{b}_R}$ comes from the mass term between b_L and $\tilde{b}_R$. Via the b_L component, the physical $\tilde{b}$ couples to W and t_L (with SM coupling $g/\sqrt{2}$). When we project onto the longitudinal W, we get a factor of E/m_W from the polarization vector, where $E \sim m_{\tilde{b}_R}$ since we are considering decays of $\tilde{b}_R$. The coupling to W_{long} is $y_t f(c_{t_R})$ as expected using the goldstone equivalence theorem (coupling to charged Higgs). To summarize, in unitary gauge, the physical $\tilde{b}_R$ has the following interactions: $\tilde{b}_R(g_{Zb_L} b_L Z + (g/\sqrt{2})\; t_L W) m_t f(c_{t_R})/m_{\tilde{b}_R}$ where $g_{Zb_L} = (g/\cos\theta_W)(1/2 - \sin^2\theta_W/3)$.

2.3 Decay widths

The partial width for the decay $\tilde{b}_R \to t_R W^-$ is

$$\Gamma_{t_R W^-} = \frac{{g_{Wtr}}^2 \left[{m_{\tilde{b}_R}}^4 + ({m_W}^2 - 2{m_t}^2){m_{\tilde{b}_R}}^2 + {m_t}^4 - 2{m_W}^4 + {m_t}^2{m_W}^2\right]}{32\pi {m_{\tilde{b}_R}} {m_W}^2} \; \lambda^{1/2}(m_t, m_W, m_{\tilde{b}_R}) \tag{4}$$

where

$$g_{Wtr} = g_R \; k\pi r_c \left(\frac{m_W}{M_{KK}}\right)^2 \quad \text{and} \quad \lambda(m_t, m_W, m_{\tilde{b}_R}) = 1 + \frac{(m_t^2 - m_W^2)^2}{m_{\tilde{b}_R}^4} - 2\frac{(m_t^2 + m_W^2)}{m_{\tilde{b}_R}^2}. \tag{5}$$

We use the same formula for the decay $\tilde{b}_R \to t_L W^-$ except that the coupling constant is replaced by

$$g_{Wtl} = f(c_{t_R}) \frac{m_t}{m_{\tilde{b}_R}} \times \frac{g}{\sqrt{2}}. \tag{6}$$

The decay width for $\tilde{b}_R \to b_L Z$ is

$$\Gamma_{b_L Z} = \frac{{g_{Zbl}}^2 \left({m_{\tilde{b}_R}}^2 - {m_Z}^2\right)\left({m_{\tilde{b}_R}}^4 + {m_Z}^2{m_{\tilde{b}_R}}^2 - 2{m_Z}^4\right)}{32\pi \; m_{\tilde{b}_R}^3 {m_Z}^2} \tag{7}$$

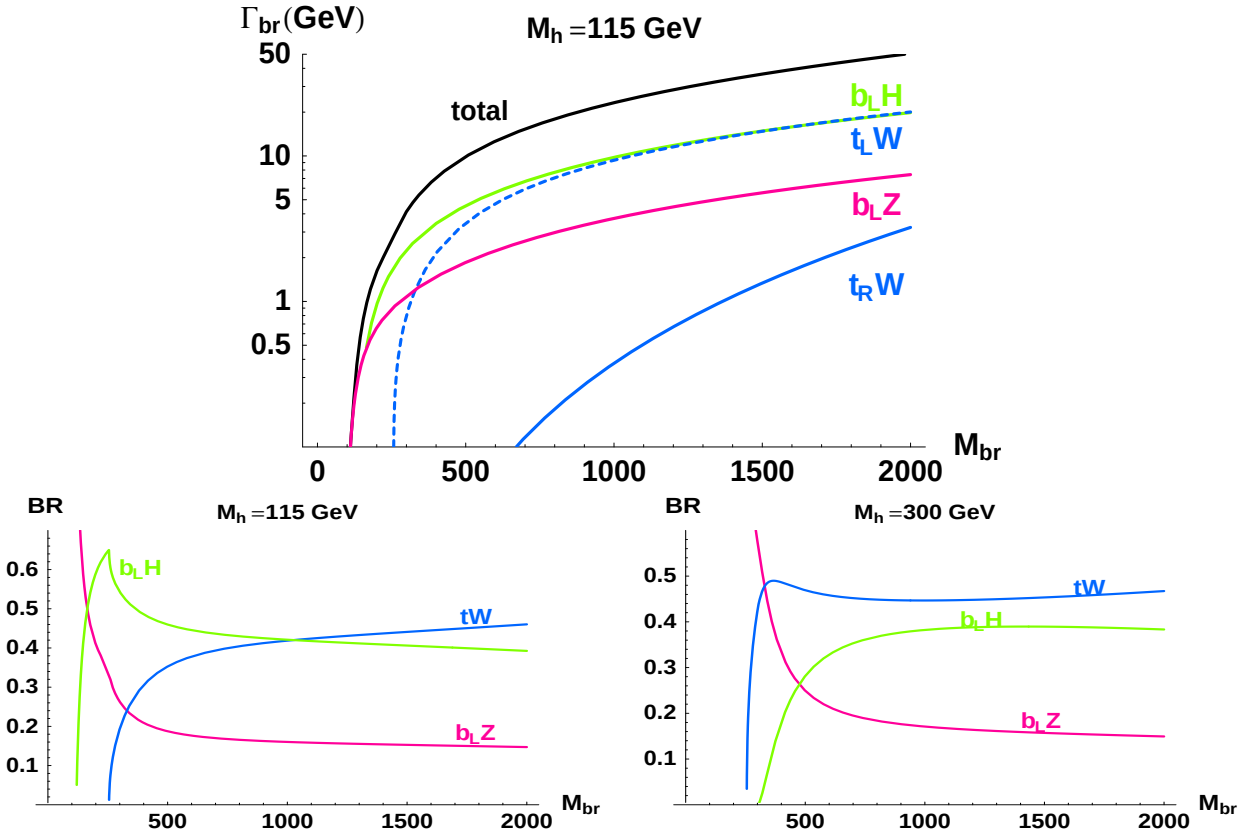

Figure 4: Decay widths of $\tilde{b}_R$ as a function of its mass and corresponding branching ratios.

where

$$g_{Zbl} = f(c_{t_R})\frac{m_t}{m_{\tilde{b}_R}} \times \frac{g}{6\cos\theta_W}[3 - 2\sin^2\theta_W], \tag{8}$$

and finally

$$\Gamma_{b_L H} = \frac{f^2(c_{t_R})\left(m_{\tilde{b}_R}{}^2 - m_H{}^2\right)^2}{32\pi m_{\tilde{b}_R}^3}. \tag{9}$$

As we said, in our analysis, we use $f(c_{t_R}) = 1$, $g_R = g$, $M_{KK} = 3$ TeV, and $k\pi r_c = \ln(10^{15})$, so that the only free parameter is $m_{\tilde{b}_R}$.

In our formulae, we have assumed that $(t_R, \tilde{b}_R)$ form an $SU(2)_R$ doublet even though we know that this is not the realistic situation. The solution to the $Zb\overline{b}$ problem indeed requires that t_R is either a singlet under $SU(2)_R$ or belongs to a $(\mathbf{1},\mathbf{3})+(\mathbf{3},\mathbf{1})$ under $SU(2)_L \times SU(2)_R$ [5]. In the first case, there is obviously no $\tilde{b}_R$. However, this does not mean that there is no associated light KK quark. Indeed, in gauge-Higgs unification models (see Ref. [21]) which are presumably the best motivated models for EW symmetry breaking in RS, the SM t_R belongs to a larger multiplet which necessarily leads to light custodian partners. In minimal composite Higgs models, t_R belongs to a **5**=((**2**,**2**),(**1**,**1**)) or a **10**=((**2**,**2**),(**1**,**3**)+(**3**,**1**)) of $SO(5)$. Its $(\mathbf{2},\mathbf{2})$ partners contain the SM Q_L as well as an extra doublet of custodians of electric charge (2/3,5/3). The Q=2/3 quark will not lead to the $4W$ signature, but the Q=5/3 quark (that we name $\tilde{q}$) will, and with a branching ratio essentially equal to 1. If t_R belongs to a **10**, there

will be as well two bottom-like custodians $\tilde{b}_R$ and $\tilde{b}_L$, and two alike $\tilde{q}$ custodians all leading to the $4W$ signature. All these particles have the same mass, so they are produced with the same cross section. The $L \leftrightarrow R$ discrete symmetry also guarantees the same couplings for $\tilde{b}_R$ and $\tilde{b}_L$ and for $\tilde{q}_R$ and $\tilde{q}_L$. However, the fact that they belong to a triplet rather than a doublet will change the couplings presented below by a Clebsh-Gordan factor of order 1. In any case, for our analysis, the total widths are not important: the $\tilde{b}_R$, $\tilde{b}_L$ and $\tilde{q}$ decay almost as soon as they are produced.

In our simulation, we have chosen to illustrate the signal in the case where t_R belongs to **(1,3)+(3,1)**. The number of $4W$ events at the end will thus be $2(1+B^2)/B^2$ times the number of events obtained from just one $\tilde{b}_R$ decaying to tW (as given in Fig. 6), where B is the relevant branching ratio.

To summarize this discussion, whatever model is being considered, there will be at least one light KK quark, related to the SM top quark, that will lead to our $4W$ signature. Additional light KK quarks will also contribute. Note also that the value of the Higgs mass depends in principle on the choice of embedding for the top and bottom quarks. In Ref. [6,18], m_H and $m_{\tilde{b}_R}$ are strongly related. Models with gauge-Higgs unification typically have a light Higgs, while for the present analysis we allow the Higgs mass to be free and as heavy as 300 GeV.

3 Preferred decays and event selection

In this study, we focus on those decay channels which show promise for being detected in the pp collisions of the LHC. First, we rely on a single isolated lepton arising from one of the W's to provide a clean and efficient trigger. We then reconstruct other W's in the event using pairs of jets. W bosons mostly decay into a pair of quarks ($BR = 67.96\%$), while they decay into a charged and neutral lepton pair about 10.68% of the time for each lepton generation.

The actual rate of multi-W events arising from our signal depends upon the $\tilde{b}_R$ mass as well as the Higgs mass: for instance, in the case of $m_{\tilde{b}_R} \lesssim 500$ GeV, the branching ratio into bZ increases dramatically from the $\sim 20\%$ characteristic of higher $\tilde{b}_R$ masses, leading to decay signatures such as 2 b jets + missing E_T, 2 b jets + 2 leptons + missing E_T, or 2 b jets + 4 leptons. We do not pursue these signatures here.

For $m_{\tilde{b}_R} \gtrsim 500$ GeV, however, the Higgs mass plays an important role. If $m_H \sim 115$ GeV, it decays mainly into b quarks, and the $\tilde{b}_R \to bH$ channel leads to 6 b jets. Since the branching ratio for bH is typically $\sim 50\%$, this takes half of the decays away. On the other hand, if the Higgs decays mainly into WW, then even the $\tilde{b}_R$ decay into bH produces the 4 W + 2 b signature. In this case, most of the produced $\tilde{b}_R$ lead to this signature. Note that we are assuming that $\tilde{b}_R$ is the lightest of the KK fermions, as this is the natural situation in minimal models. However, it could happen, such as in the GUT models of Ref. [7,8], that there are lighter KK states such as the KK RH neutrino. The Higgs would then mainly decay into this KK RH neutrino, the $H \to WW$ branching ratio would practically vanish, and we would lose the possibility of increasing the WW yield from the Higgses.

If the Higgs mass is in the region where the dominant decay is actually to WW^*, the visible signal rate will also be reduced, since $W^* \to jj$ will not peak very much around the W mass. Of course, if $W^* \to l^-\nu$ and $W \to jj$, we still get our trigger and our W combination. For $m_H > 300$ GeV, $H \to WW \to l\nu jj$ becomes significant, so $m_H = 300$ GeV is a suitable choice for a first look at multi-W signatures. The branching fraction of $H \to WW$ is about

70% in the m_H region of 200 to 350 GeV, where the $t\bar{t}$ channel opens up.

It should also be noted that in a typical detector, it is not trivial to measure the charge of a jet's precursor; moreover, the jet energy is reconstructed with a finite resolution. For instance, for dijet pairs with $p_T > 350$ GeV, the ATLAS Technical Design Report [22] claims a mass resolution of 6.9 GeV, which is not much less than the difference between the W and Z masses. The two mass peaks will overlap significantly, and indeed may be seen as a single bump. The proposed detection method will therefore have difficulty differentiating genuinely $WWWW$ events from, for instance, $WWZZ$ arising from a $\tilde{b}_R$ decaying to bH, followed by $H \to ZZ$. For the purpose of discovering $\tilde{b}_R$, it is not clear that there is any advantage in discriminating between W's and Z's here. In the present signal simulation, we do not consider these possibilities, but in principle, we should simulate these other decays as they can potentially increase our signal.

3.1 Backgrounds

The Standard Model background for $4W$ production (see Ref. [15, 16]) is suppressed by high powers of electroweak couplings and we neglect it. The dominant background is actually fake and comes from the misinterpretation of jets as coming from W's. The two important backgrounds we consider arise from $t\bar{t}$ and $t\bar{t}H$ production. $t\bar{t}$ leads to 2 W's and 2 b's with four extra jets misinterpreted as coming from hadronic decays of W's. At large Higgs mass, where the Higgs decays primarily into WW, $t\bar{t}H$ exactly leads to $4W$ + 2-b-jets and becomes a serious background for heavy $\tilde{b}_R$ masses: if $m_{\tilde{b}_R} \sim 1$ TeV, the two production cross sections are comparable [23]. Distinguishing the signal in this case would be a significant challenge.

Diboson EW production can also contribute by misidentification and event overlaps. However, the LHC production cross sections for these processes are smaller with respect to $t\bar{t}$ production. In addition, they do not produce a pair of high p_t b-jet pairs. Therefore, contributions from such processes are not currently estimated. A list of diboson production cross sections taken from Ref. [24] are listed below along with that of $t\bar{t}$ as taken from the ATLAS Technical Design Report and references therein [22, 25]:

$t\bar{t}$	833 pb (NLO + NLL resummation)
W^+W^-	86.7 pb
WZ	32.4 pb
ZZ	12.9 pb

The cross section for $gg \to t\bar{t}WW$ is 4 orders of magnitude below that of $t\bar{t}$ and this background is neglected. Similarly, the $4W + 4b$ background from $(t\bar{t})(t\bar{t})$ production can be neglected as it is more than 4 orders of magnitude smaller than the $t\bar{t}$ cross section: the phase space volume is scaled down by a $1/(4\pi)^4$ factor and there is a g_s^4 suppression factor in the cross section. In the end, this is $\alpha_s^2/(4\pi)^2$ suppression compared to the $t\bar{t}$ cross section. This is consistent with the cross section obtained with Comphep: 1.3×10^{-2} pb just from the gg contribution.

Finally, there are of course Standard Model EW processes which give W + 6-jet events, but these are of higher order, and in addition they have no b jets so we ignore them. There are also QCD processes which will give a hard photon + 6 jets, with the photon converting to a high-p_T lepton. Such events should not have much missing E_t and so should also be suppressed.

4 Signal and background simulation

The Lagrangian of the model is implemented into CalcHEP (v2.4.3 [26]), a tree level Monte Carlo event generator that can deal with multi-particle final states. We generate $t\bar{t}WW$ events from $\tilde{b}_R$ pair production in CalcHEP, which are further processed in PYTHIA 6.4.01 [27].

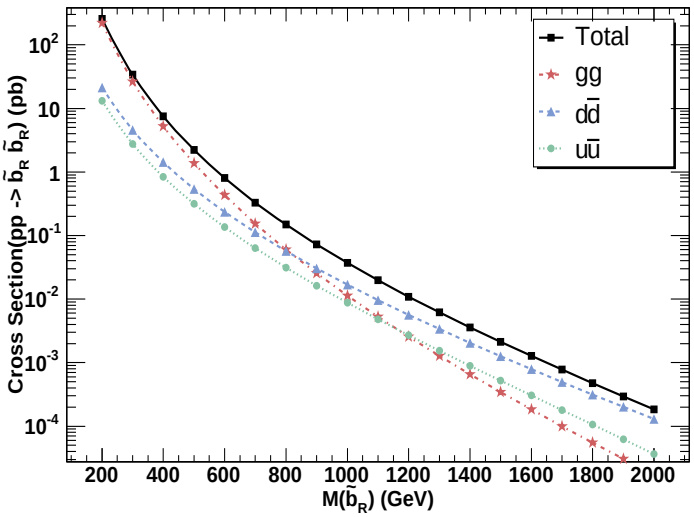

Figure 5: Pair production cross section for $\tilde{b}_R$ at the LHC. Only masses above the $t + W$ threshold are considered.

Figure 5 shows the $\tilde{b}_R$ pair production cross section at the LHC. We use CTEQ6L parton distribution functions and consider only the contribution from light quarks, u and d. The dominant contribution comes from the gluon-initiated hard scattering up to about a $\tilde{b}_R$ mass of 800 GeV. The QCD scale was set to the mass of $\tilde{b}_R$. The cross sections include the contributions from s-channel EW exchange diagrams, though the combined contribution from these channels is negligibly small. For example, for $\tilde{b}_R$ mass of 500 GeV, the contribution from EW channels is about three orders of magnitude smaller than those involving the QCD coupling.

Figure 6 shows the $4W + 2b$ final states expected in 10fb^{-1} of LHC data as a function of the $\tilde{b}_R$ mass, for two Higgs masses and considering only the production cross section and branching fractions. For a $\tilde{b}_R$ mass of 500 GeV, the yields are about 5000 events from tW and 900 from bH for a Higgs mass of 300 GeV. The yield is about 2800 events from only the tW channel for a Higgs mass of 115 GeV, with no contribution from the bH channel.

As discussed in Section 2.3, there are additional exotic quarks with exactly the same properties as $\tilde{b}_R$ which therefore enhance the total number of events: for $m_{\tilde{b}_R} = 500$ GeV and $m_H = 300$ GeV, including $\tilde{b}_{R,L}$ and $\tilde{q}_{R,L}$, this multiplying factor amounts to 11.2. In the case of the models discussed in Ref. [6, 18–20], where some have only one light $Q = 5/3$ quark $\tilde{q}$ instead of $\tilde{b}_R$, this factor is $1/B^2 = 4.6$.

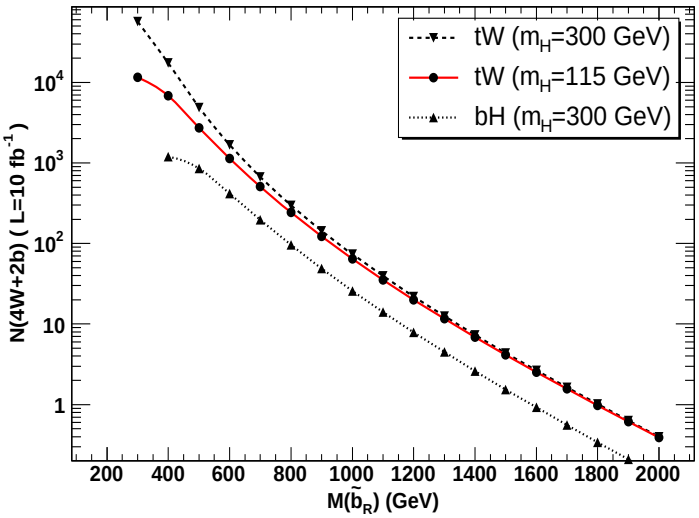

Figure 6: Number of $4W + b\overline{b}$ events expected from the tW and bH decays of $\tilde{b}_R$ for 10 fb^{-1} of LHC data.

4.1 Trigger strategy and event reconstruction

In order to investigate how such events could be examined using an LHC detector such as ATLAS, we first restrict ourselves to simulating $\tilde{b}_R$ pair production and their decays through the tW channel. For the present model analysis, we choose $m_{\tilde{b}_R} = 500$ GeV and $m_H = 300$ GeV. We apply event filters and acceptance criteria based on nominal ATLAS parameters as found in the Technical Design Report [22]. The following "trigger", applied to the generated events, is based on the lepton criteria for selecting $W \to \ell\nu$ events: at least one electron or muon with $p_T > 25$ GeV must be found within the pseudorapidity range $|\eta| < 2.4$, where $\eta = -\ln\tan(\theta/2)$ and θ is the angle relative to the pp collision axis; then, the "missing E_T", calculated by adding all the neutrino momenta in the event and taking the component transverse to the collision axis, must exceed 20 GeV.

We mimic cone-based hadronic jets as they might be observed in a detector: stable charged and neutral particles within $|\eta| < 4.9$ (the range of the ATLAS hadronic calorimeter), excluding neutrinos, are first ranked in p_T order. Jets are seeded starting with the highest p_T tracks, with $p_T > 1$ GeV; softer tracks are added to the nearest existing jet, as long as they are within $\Delta R < 0.4$ of the jet centroid, where $\Delta R = \sqrt{\Delta\phi^2 + \Delta\eta^2}$. The number of jets with $p_T > 20$ GeV is shown in Figure 7. The signal is peaked around 8 jets. Additional jets can be produced in quark hadronization and underlying parton activity, while jets can be lost due to falling below the energy threshold or outside the geometric acceptance.

The background sample is dominated by $t\overline{t}$ events generated using TopRex (version 4.11) [28] and PYTHIA (version 6.403), with CTEQ6L parton distribution functions. The small $t\overline{t}H$ contribution to the background has been modelled with PYTHIA. As expected, the background has fewer high-p_T jets than the signal, peaking around 5 jets.

Figures 8 and 9 compare signal and background distributions for transverse momenta of generated particles as well as event-level observables such as the "trigger" (highest-p_T) lepton p_T, missing E_T, and scalar sum of the E_T's of all the jets in the event.

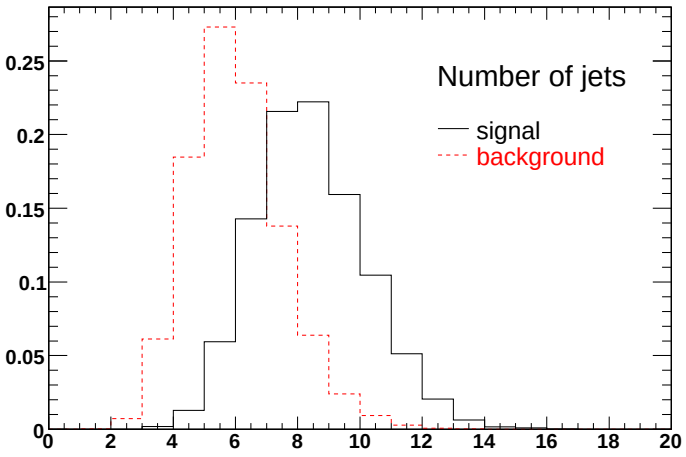

Figure 7: Number of jets with $p_T > 20$ GeV for signal and background. Both distributions are normalized to unit area.

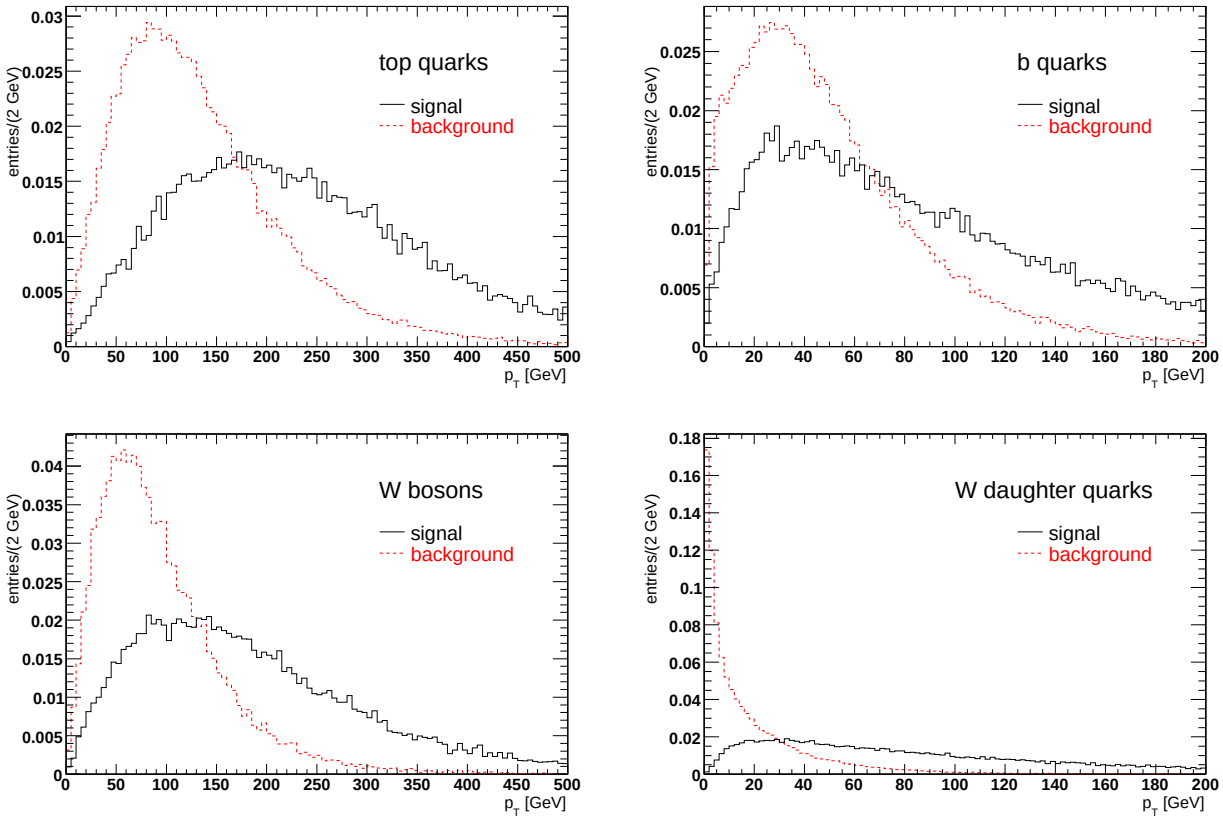

Figure 8: Generator-level signal and background p_T distributions after the "trigger" conditions, normalized to unit area. Top left: t quarks. Top right: b quarks. Bottom left: W bosons. Bottom right: W daughter quarks.

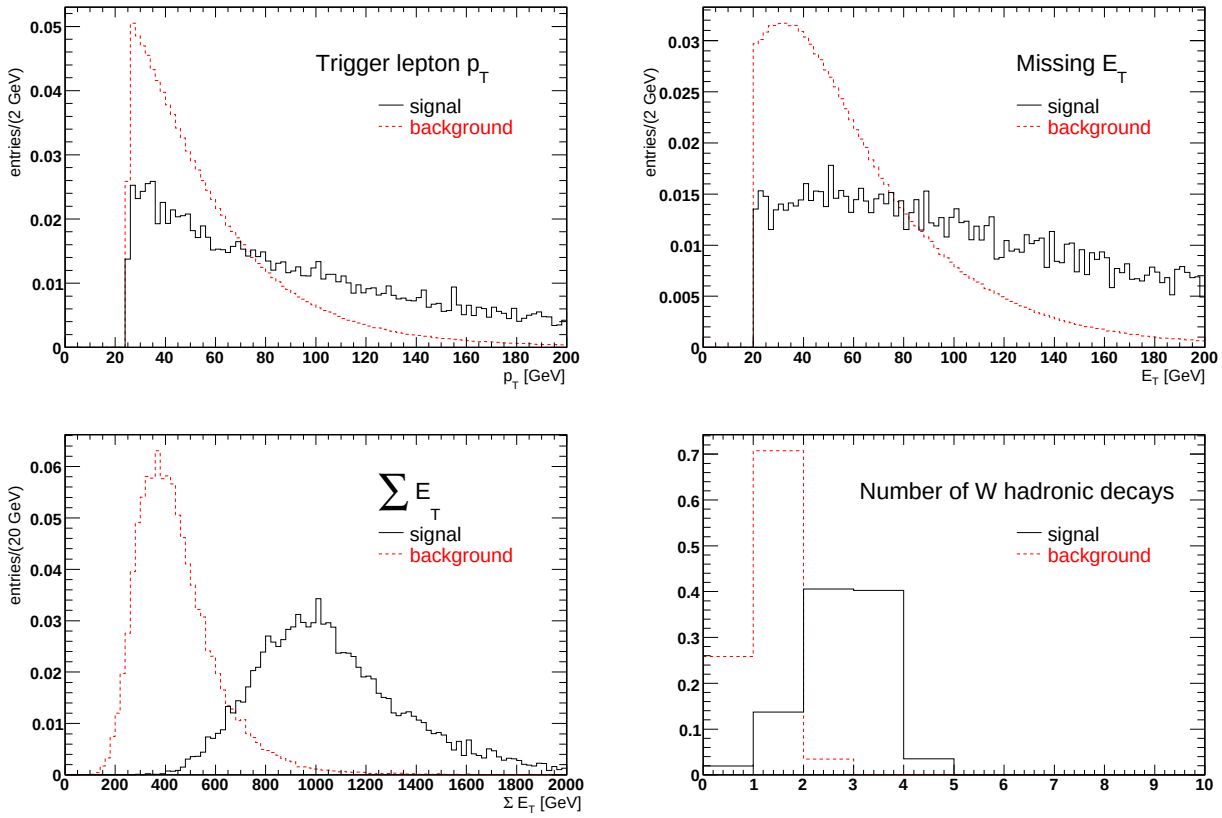

Figure 9: Generator-level signal and background "trigger" distributions after initial trigger conditions, normalized to unit area. Top left: p_T of stiffest electron or muon. Top right: missing E_T. Bottom left: scalar sum of E_T in the event. Bottom right: number of W's decaying hadronically in the event.

The scalar E_T sum distribution in Figure 9 (bottom left) suggests that the background can be significantly reduced by requiring the sum to exceed 800 GeV. We also restrict the analysis to events with between 6 and 9 jets. No b jet tagging is performed at this point.

After applying the 800 GeV cut to the scalar E_T sum, we construct hadronic W candidates by adding the 4-momenta of two jets, each with $p_T > 20$ GeV and assuming that each individual jet has zero mass. Since the W's are typically produced with $p_T > 150$ GeV, as shown in Figure 8, the total p_T of the dijet combination is further required to exceed that value. The mass spectrum for the signal and background events, representing 10 fb^{-1} of LHC data, is shown in Figure 10. We have scaled up the signal to include the $\tilde{b}_L$ and $\tilde{q}$ relatives of the $\tilde{b}_R$, as discussed in Section 2.3 (this scaling assumes charge-symmetric lepton and jet identification). A prominent peak can be seen around 80 GeV with width 5 GeV. The width is due to, among other effects, the hadronization of the daughter quarks, with the resulting jets sometimes overlapping with other activity in the event. The low mass of the peak, relative to the generated W mass, is expected given, for instance, the finite cone size of the jets. A W peak is also evident in the $t\bar{t}$-dominated background distribution, as expected. Figure 10 also shows the reduction in the signal's combinatorial background if perfect b tagging is achieved, though experimentally, b tagging is rarely very efficient or pure.

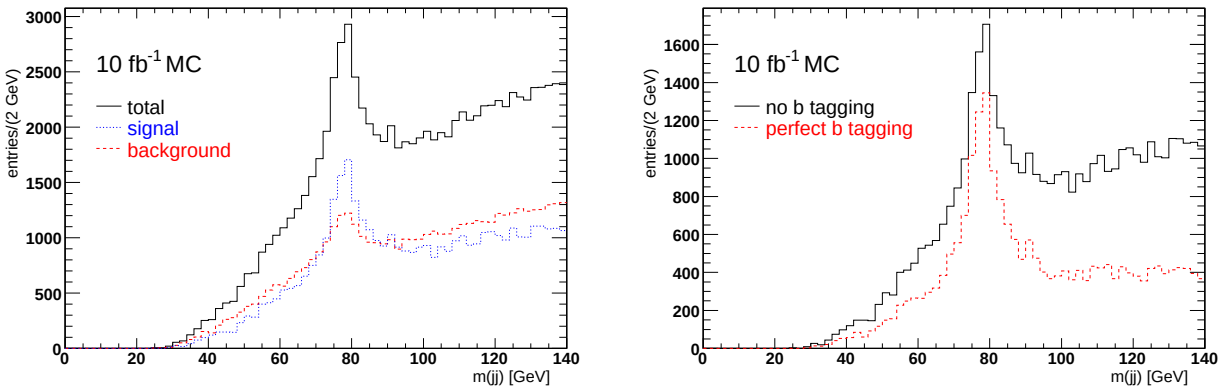

Figure 10: Left: dijet mass distribution for all jets for signal, background, and their sum, for 10 fb^{-1} integrated luminosity. Right: comparison of dijet mass distributions before and after eliminating all b jets. The black histogram here is the same as the blue in the figure to the left.

In order to suppress the most common ($t\bar{t}$) Standard Model background, we eliminate the single hadronic W decay in the following manner: we start with the highest p_T jet and search among the lower p_T jets for a combination whose mass falls between 70 and 90 GeV. If no combination is found, the search is continued using the next highest p_T jet. If a pair is found, those two jets are removed for consideration in forming the subsequent dijet mass combinations, which are shown in Figure 11. The observable peak is by now dominated by the signal, though the background peak has not been entirely eliminated. These background events might appear, paradoxically, to contain 3 W's, one decaying leptonically and two hadronically, but a more mundane explanation is that the trigger lepton and missing energy actually arise from semileptonic b decay occurring among the far more numerous $t\bar{t}$ events. These events also appear in Figure 9 (bottom right) as background events with 2 hadronic W

decays; a similar fraction of signal events contain 4 hadronic W decays. While the background peak may not be very large compared to the signal, it can still be further suppressed by increasing the trigger thresholds.

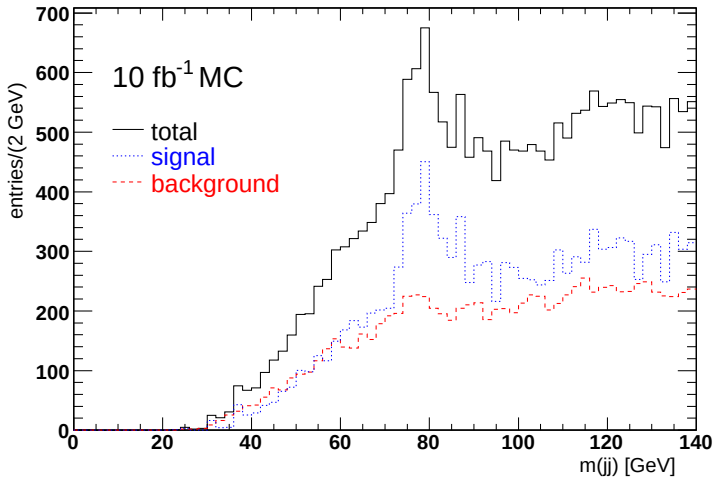

Figure 11: Dijet mass distribution and signal, background, and their sum, after eliminating the first hadronic W candidate. The distribution represents 10 fb^{-1} integrated luminosity.

Relating the $\tilde{b}_R$ production cross section to the size of the peak (and therefore the discovery potential of this signature) is non-trivial: first, we would have to subtract or suppress the $t\bar{t}$ component, model the dijet mass resolution, and calculate the reconstruction efficiency in light of the multiple W decays in the event. Such details are best reserved for further investigation, when a more detailed and specific simulation of the detector and experimental environment, including the effects of detector material and multiple pp interactions in a beam crossing, can be employed. Furthermore, the relationship between $\tilde{b}_R$ production and yield is complicated by the m_H-dependent interplay of different decay modes and how they contribute W's and Z's to the signal. However, this initial analysis, indicative of the kind which could be attempted at an LHC experiment, suggests that it will be possible to distinguish the signal from the major physics backgrounds.

4.2 Further analysis directions

It has been suggested in Ref. [18] that if all four W's decay leptonically, the resulting "golden" signature of 4 leptons + $b\bar{b}$ + missing E_T would have very little SM background. As shown in Figure 12, however, the rate for this signature would be suppressed by approximately two orders of magnitude relative to a signature requiring only one leptonic W decay. At the same time, because of the multiple neutrinos, it would be difficult to identify the leptons as W daughters. As a result, while this signature could be indicative of new physics, it would be difficult to distinguish what kind of new physics is being observed.

An important piece of corroborative evidence for these models is the observation of the custodian quark $\tilde{q}$ carrying electric charge $Q = 5/3$. Pair production of this quark would lead to exactly the same 4 W + $b\bar{b}$ final state as the $\tilde{b}_R$. A possible method to distinguish the

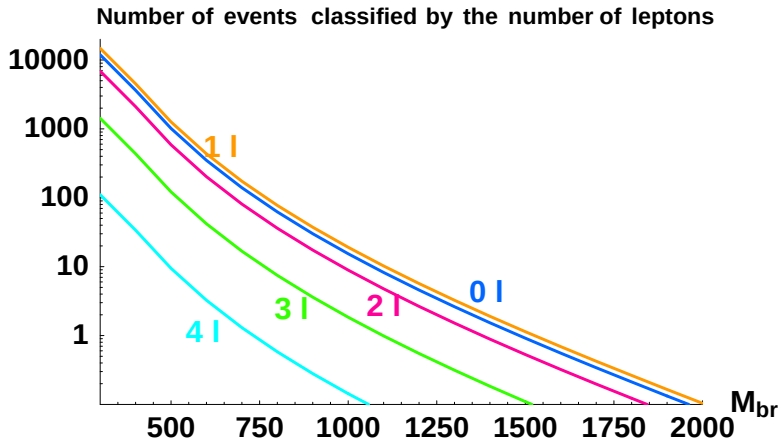

Figure 12: Number of $4W$ events (coming from $\tilde{b}_R$ only) in the case $m_H = 300$ GeV, with the assumption of 10 fb^{-1} integrated luminosity. Leptons are either e or μ.

$\tilde{q}$ events is to select events with two high-p_T leptons with the same sign (presumably from the two W's from a single $\tilde{q}$), and then fully reconstruct the other $\tilde{q}$ in the event through its $tW \to bWW \to bjjjj$ decay. This method is driven by the typical situation that the charge of an observed lepton can be measured reliably, while that for a jet cannot. The fully reconstructed $\tilde{q}$ would yield a narrow peak in the $b + 4$ jet combined invariant mass distribution, while the corresponding distribution arising from $\tilde{b}_R$ pair production and decay would be much broader. The main disadvantage of this method is the typically low efficiency of a full reconstruction, which requires all decay products to be observed and well measured. We therefore expect that confirming the existence of the $\tilde{q}$ custodian would require rather more data than the 10 fb^{-1} studied here (note, however, that the LHC's design luminosity would yield 100 fb^{-1} per year).

Finally, let us note that one could also consider the single production of $\tilde{b}_R$ together with the standard b quark via s-channel Z or W-gluon fusion, or together with the top quark via s-channel W. This would be especially relevant for large $\tilde{b}_R$ masses and would deserve a separate study.

5 Conclusion and future prospects

We have studied new signals in pair production of heavy $Q = -1/3$ and $Q = 5/3$ quarks at the LHC. They are produced through standard QCD interactions with a cross section $\sim \mathcal{O}(10)$ pb for masses of several hundreds of GeV. Heavy quarks such as $\tilde{b}_R$ are well-motivated in Randall–Sundrum models with custodial symmetry. They are generally Kaluza-Klein partners of the Standard Model Right-Handed top quark. Their decay channels were described in detail in this paper. In the present work, we focussed on the 4-W events which we believe are quite specific to this class of models, and also experimentally promising. We have considered the process $gg, q\overline{q} \to \tilde{b}_R\overline{\tilde{b}}_R \to W^-t\ W^+\overline{t} \to W^-W^+b\ W^+W^-\overline{b}$ where at least one W boson decays leptonically and the other ones hadronically. A simulation of this signal and its main background was performed, and an analysis strategy outlined which distinguishes the signal

from the sizable Standard Model backgrounds. The peak we obtain in the dijet mass distribution suggests that it is possible to reach a signal significance beyond the 5σ level. Further study with more detailed simulation is required to map the discovery potential for this signal at an LHC experiment such as ATLAS, or at the ILC, and to connect the observable signal to the production cross section.

Acknowledgments

We acknowledge the financial support of the Particle Physics and Astronomy Research Council of the United Kingdom. We are indebted to Kaustubh Agashe for collaboration and many helpful discussions. We also thank Sasha Pukhov and Geneviève Bélanger for checking the Comphep file and especially S. Pukhov for valuable help on CalcHEP related questions. G.S is grateful to Henry Frisch and Drew Fustin for collaboration at some very early stage of this project. Finally, G.S thanks Roberto Contino for useful comments.

References

[1] L. Randall and R. Sundrum, Phys. Rev. Lett. **83**, 3370 (1999) [arXiv:hep-ph/9905221].

[2] K. Agashe, A. Delgado, M. J. May and R. Sundrum, JHEP **0308**, 050 (2003) [arXiv:hep-ph/0308036].

[3] N. Arkani-Hamed, M. Porrati and L. Randall, JHEP **0108**, 017 (2001) [arXiv:hep-th/0012148]. R. Rattazzi and A. Zaffaroni, JHEP **0104**, 021 (2001) [arXiv:hep-th/0012248].

[4] C. Csaki, C. Grojean, L. Pilo and J. Terning, Phys. Rev. Lett. **92**, 101802 (2004) [arXiv:hep-ph/0308038]. G. Cacciapaglia, C. Csaki, G. Marandella and J. Terning, arXiv:hep-ph/0607146.

[5] K. Agashe, R. Contino, L. Da Rold and A. Pomarol, arXiv:hep-ph/0605341.

[6] R. Contino, L. Da Rold and A. Pomarol, arXiv:hep-ph/0612048.

[7] K. Agashe and G. Servant, Phys. Rev. Lett. **93**, 231805 (2004) [arXiv:hep-ph/0403143].

[8] K. Agashe and G. Servant, JCAP **0502**, 002 (2005) [arXiv:hep-ph/0411254].

[9] K. Agashe, G. Perez and A. Soni, arXiv:hep-ph/0606293; K. Agashe, A. Belyaev, T. Krupovnickas, G. Perez and J. Virzi, arXiv:hep-ph/0612015.

[10] J. A. Aguilar-Saavedra, Phys. Lett. B **625**, 234 (2005) [Erratum-ibid. B **633**, 792 (2006)] [arXiv:hep-ph/0506187]. J. A. Aguilar-Saavedra, PoS **TOP2006**, 003 (2006) [arXiv:hep-ph/0603199].

[11] G. Azuelos *et al.*, Eur. Phys. J. C **39S2**, 13 (2005) [arXiv:hep-ph/0402037]; M. Carena, J. Hubisz, M. Perelstein and P. Verdier, arXiv:hep-ph/0610156.

[12] M. S. Chanowitz and M. K. Gaillard, Phys. Lett. B **142**, 85 (1984).

[13] M. Golden and S. R. Sharpe, Nucl. Phys. B **261**, 217 (1985).

[14] D. A. Morris, R. D. Peccei and R. Rosenfeld, Phys. Rev. D **47**, 3839 (1993) [arXiv:hep-ph/9211331].

[15] V. D. Barger, T. Han and H. Pi, Phys. Rev. D **41**, 824 (1990).

[16] V. D. Barger, A. L. Stange and R. J. N. Phillips, Phys. Rev. D **45**, 1484 (1992).

[17] F. Gianotti, M.L. Mangano, T. Virdee, Eur. Phys. J **C39**, 293 (2005).

[18] M. Carena, E. Ponton, J. Santiago and C. E. M. Wagner, arXiv:hep-ph/0607106; arXiv:hep-ph/0701055.

[19] A. Djouadi, G. Moreau and F. Richard, arXiv:hep-ph/0610173.

[20] G. Cacciapaglia, C. Csaki, G. Marandella and J. Terning, arXiv:hep-ph/0611358.

[21] R. Contino, Y. Nomura and A. Pomarol, Nucl. Phys. B **671**, 148 (2003) [arXiv:hep-ph/0306259].

[22] ATLAS Detector and Physics Performance. Technical Design Report, Volumes 1 and 2, CERN-LHCC-99-14, CERN-LHCC-99-15, May 1999.

[23] S. Dawson, L. H. Orr, L. Reina and D. Wackeroth, Phys. Rev. D **67**, 071503 (2003) [arXiv:hep-ph/0211438].

[24] J. M. Campbell and R. K. Ellis, Phys. Rev. D **60**, 113006 (1999) [arXiv:hep-ph/9905386].

[25] R. Bonciani, S. Catani, M. L. Mangano and P. Nason, Nucl. Phys. B **529**, 424 (1998) [arXiv:hep-ph/9801375].

[26] A. Pukhov, arXiv:hep-ph/0412191.

[27] T. Sjostrand, S. Mrenna and P. Skands, JHEP **0605**, 026 (2006) [arXiv:hep-ph/0603175].

[28] S. R. Slabospitsky and L. Sonnenschein, Comput. Phys. Commun. **148**, 87 (2002) [arXiv:hep-ph/0201292].